ISSN: 1410-8917
Jurnal Kimia Sains & Aplikasi
e-ISSN: 2597-9914

Jurnal Kimia Sains dan Aplikasi 28 (9) (2025): 522-528

Jurnal Kimia Sains dan Aplikasi
Journal of Scientific and Applied Chemistry

Journal homepage: http://ejournal.undip.ac.id/index.php/ksa

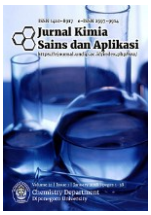

Effect of Carbonization Step on Surface Character of Activated Carbon from Cassava Peels and Its Simple Application for BTEX Adsorption

Cucun Alep Riyanto [1,*], Alvama Pattiserlihun [2], Blessy Yemima Andiani [1], Ezra Kurniawan [1], Fahmi Puteri Perdani [1], Marcelino Kelpitna [3]

[1] Department of Chemistry, Faculty of Science and Mathematics, Satya Wacana Christian University (UKSW), Salatiga, Indonesia
[2] Department of Physical Education, Faculty of Science and Mathematics, Satya Wacana Christian University (UKSW), Salatiga, Indonesia
[3] BMT Laboratory, Bogor, Indonesia

* Corresponding author: cucun.riyanto@uksw.edu

https://doi.org/10.14710/jksa.28.9.522-528

Article Info

Article history:

Received: 13th June 2025
Revised: 20th November 2025
Accepted: 25th November 2025
Online: 8th December 2025

Keywords:
Activated Carbon; Cassava Peel; Carbonization; Pore Distribution; Volatile Organic Compound

Abstract

Activated carbon is obtained from biomass waste because it is cheaper and renewable from an environmental perspective. In cassava peel biomass waste, it is necessary to study the effect of the carbonization stage on the surface character and pore distribution of the activated carbon obtained. In this research, the study of the impact of the carbonization stage is continued with the application of adsorption to volatile compounds, specifically benzene, toluene, ethylbenzene, and xylene (BTEX). This study conducted carbonization at 400°C (t: 60 minutes) followed by dual activation stages, namely chemical activation (carbon: H_3PO_4 30%, ratio 1:5, w/b) and physical activation (furnace, T: 600°C, t: 60 minutes). After that, the activated carbon from cassava peels (CPAC) was applied as an adsorbent for BTEX. The results showed that CPAC has an amorphous character with O-H, C-H, C≡C, C=C stretching, C-O, and C=N functional groups. The carbonization step changes pore properties. CPAC-202 (with carbonization) has a mesoporous character with a surface area up to 198.233 m^2/g, with the surface dominated by C and O elements. The selectivity of BTEX gas adsorption is more significant for toluene using CPAC-202, with the best adsorption reaching 6.418 mg/L.

1. Introduction

Activated carbon is well known as an adsorbent despite various other applications, mainly due to their nature of being highly porous nature with a large surface area to facilitate adsorption [1]. Activated carbon can be produced from a variety of raw materials, such as biomass waste from agricultural products [2]. Agricultural biomass waste used as a material for making activated carbon has the advantage of being cheaper, easier to use, and renewable in environmental aspects [3]. This is based on its high economic value and the presence of chemical compounds in agricultural waste. One of the agricultural wastes that has received special attention is cassava peel.

In some processing countries, cassava peels pose a disposal challenge as waste from staple foods [4]. Cassava peel (*Manihot esculenta* Crantz) accounts for 10-20% of the total weight of cassava, making it a potential candidate for utilization in biotechnology and on an industrial scale [5]. The hemicellulose content of 23.9% and the lignin content of 7.5% [6] indicate that cassava peels exhibit a significant ability as a metal-binding material from aqueous solutions [7]. Based on FAO data in 2018, Indonesia became the third-largest cassava-producing country in the world, with production reaching 25 million tons by the end of 2015 [6], indicating significant potential for developing activated carbon sources from cassava peels. The activated carbon derived from biomass, such as cassava peels, is highly regarded for its renewability, environmental friendliness, and broad potential for applications [8].

One of the stages in the manufacture of activated carbon is the activation process, because this stage is used to enlarge the sorption area and pore volume in activated carbon [9]. Activator substances such as $ZnCl_2$ and H_3PO_4 are commonly used for materials containing lignocellulose [10]. According to Jaria *et al.* [11], H_3PO_4 has several advantages over other chemical activators, such as being friendly to the environment, requiring low energy in the activation process, and being economical (eco-friendly). H_3PO_4 activator also produces higher yields of activated carbon and has non-toxic properties, making it safe for use in the food and pharmaceutical industries [12]. Nicha *et al.* [13] was synthesized the activated carbon derived from palm shells treated with 10% H_3PO_4, the material produced larger and cleaner pores due to the effective removal of surface residues.

Another stage in the activated carbon fabrication process is carbonization. Carbonization is a physical activation process used to remove water and volatile matter from biomass, and pore formation by the formation of CO_2 and heat [2, 14]. During the carbonization process, volatile matter decreases, and fixed carbon increases [15]. Research El-Hendawy *et al.* [16] conducted carbonization at 500°C and continued chemical activation and pyrolysis at 700°C to produce activated carbon with a high surface area that has good adsorption capacity for methylene blue and Pb^{2+}. Further analysis is needed to know about the impact of the carbonization process on pore formation and the surface characteristics of the material.

Activated carbon, with its large surface area, has the potential to be used as an adsorbent for volatile organic compounds (VOCs). The adsorption method is considered more economical and environmentally friendly than other methods, such as catalytic degradation, biodegradation, and membrane technology [17]. Research by Wu *et al.* [18] on toluene adsorption using Fe-modified activated carbon fiber resulted in a toluene adsorption capacity of 218.12 mg/g. Apart from toluene, VOC adsorption can also be carried out on BTEX (benzene, toluene, ethylbenzene, and xylene) using activated carbon from eucalyptus leaves, which has a surface area of 128 m^2/g and is effective as a BTEX adsorbent, achieving a removal efficiency of 94% [19]. BTEX is commonly found in the environment, primarily due to industrial activities and the use of fossil fuels. These compounds are highly volatile, meaning they can easily vaporize into gas at room temperature, making them a significant air pollutant, especially in areas close to industrial activity, such as the petroleum industry and factories with chimneys [20].

Based on several studies conducted, this research specifically examines the effect of the carbonization stage on the surface characteristics and pore distribution of activated carbon derived from cassava peels (CPAC) biomass waste. The CPAC obtained is then used as a BTEX adsorbent to determine the significance of the carbonization stage.

2. Experimental

2.1. Tools and Instruments

The tools used in this study were a balance analytical with an accuracy of 0.01 g (Ohaus TAJ601), an analytical balance with an accuracy of 0.1 mg (Ohaus PA214), a pH meter (Hanna HI 9812), a furnace (Vulcan A-550), an oven, a grinder, a 30 and 60 mesh sieve, a porcelain cup, a reflux device, and a vacuum Buchner.

The instruments used to characterize the activated carbon results were a Fourier Transform Infrared spectrophotometer (FTIR, Shimadzu Prestige 21, Gadjah Mada University), an X-ray Diffractometer (XRD, PANalytical X'Pert Pro, State University of Malang), a Scanning Electron Microscope (SEM, Phenom Dekstop ProXL, Islamic University of Indonesia), a Surface Area Analyzer (SAA, Quantachrome NOVA 1200e, Semarang State University), and Gas Chromatography with Flame Ionization Detection (GC-FID, Agilent Technologies GC Model 7890A, PT. ALS Indonesia - Bogor).

2.2. Materials

Cassava peels were obtained from the Ledok Cassava Industry Center in Salatiga. The chemicals used included distilled water from the Chemistry Laboratory of Satya Wacana Christian University (UKSW), commercial activated carbon purchased from chemical suppliers, and H_3PO_4, NaOH, and HCl, all of which were PA-grade (Pro-Analysis) reagents from E-Merck, Germany. The BTEX stock standard solution (1000 mg/L) from the Absolut Standard was obtained from ALS Laboratory, Bogor.

2.3. Raw Material Preparation

The cassava peels were cleaned of soil or impurities, and then the white part was separated from the outer skin. The white part was washed with clean water, cut into small pieces (4 × 4 cm), and then dried in the sun for 2 days. After 2 days of drying, the samples were oven-dried at 110°C for 24 hours. The dried samples were then pulverized with a grinder and sieved using a 30-mesh sieve [21].

2.4. Carbonization and Activation Process

In the stage without carbonization, the sieved samples were impregnated with 30% H_3PO_4, using a carbon: phosphoric acid impregnation ratio of 1:5 (w/w) for 24 hours. The impregnation results were then filtered and oven-dried at 110°C for 24 hours. Afterward, they were activated in a furnace for 1 hour at an activation temperature of 600°C. The activated carbon was neutralized with a 1 M NaOH solution and rinsed with distilled water until the pH reached 7. The activated carbon was then oven-dried at 110°C for 24 hours and then stored and labeled CPAC-201 (without carbonization) [22].

At the carbonization stage, the sieved samples were carbonized in a furnace at 400°C for 1 hour. The carbonization results were cooled to room temperature, and then the carbon was activated using a 30% H_3PO_4 solution with a carbon-to-phosphoric acid impregnation ratio of 1:5 (w/w) for 24 hours. The impregnated carbon

was then filtered, oven-dried at 110°C for 24 hours, and put back in the furnace at 600°C for 1 hour. The activated carbon was neutralized with a 1 M NaOH solution and rinsed with distilled water until the pH reached 7. The activated carbon was then oven-dried at 110°C for 24 hours and stored and labeled CPAC-202 (with carbonization) [21, 23, 24].

2.5. Material Characterization

The analysis of functional groups in CPAC was conducted using FTIR within the wavenumber range of 4000–400 cm^{-1}. The crystal properties of CPAC were examined using XRD. Surface morphology was analyzed using an SEM to observe surface structures, while pore size and distribution were evaluated using an SAA.

2.6. Adsorption of BTEX

The BTEX adsorption process was conducted according to NIOSH Method 1501 for hydrocarbons and aromatic compounds. A personal air sampling pump (Gilibrator DBX II), calibrated to operate at a flow rate of 0.01–2 L/min, was used in the setup. The adsorbents employed were CPAC-201 and CPAC-202. A total of 1 g of each adsorbent was placed into a BTEX adsorption simulator and connected via tubing to the personal pump set to a specific flow rate. The adsorption process was conducted during the evaporation of 1 mL of a standard BTEX solution (purged with N_2), prepared in varying concentrations. After the adsorption process, the BTEX compounds were desorbed from the adsorbent using CS/DCM, and the concentrations were then analyzed using GC-FID.

Gas chromatography analysis was performed using an Agilent Technologies GC Model 7890A equipped with a Flame Ionization Detector (FID). The injector (A) was set at 225°C, and the detector (FID-A) at 250°C. The column used was HP-1 MS (30 m × 320 µm × 0.25 µm). Nitrogen was used as the carrier gas at a flow rate of 2.5 mL/min. The oven temperature program began at 40°C (held for 1 minute), followed by Ramp 1 at 10°C/min for 8 minutes, and Ramp 2, which reached a final temperature of 120°C and was held for 2 minutes, resulting in a total run time of 11 minutes. The nitrogen purge for the septum was maintained at 3 mL/min. The injection volume was 1 µL.

3. Results and Discussion

3.1. FTIR Characterization of CPAC

The FTIR results shown in Figures 1b and 1c display absorption peaks at wavenumbers 3425.58, 2931.80, 2337.72, 1620.21, and 1157.29 cm^{-1}, corresponding to the vibrations of O–H, C–H, C≡C, C=C stretching, and C–O stretching, respectively [25]. These peaks are similar to those observed in commercial activated carbon (CAC). Additionally, Figures 1b and 1c exhibit a broader peak at 1566.20 cm^{-1} compared to Figure 1a, indicating the presence of C=N stretching vibrations, which are associated with cyanide compounds found in cassava peel [26]. The identified functional groups and their respective absorption regions in the activated carbon samples are summarized in Table 1.

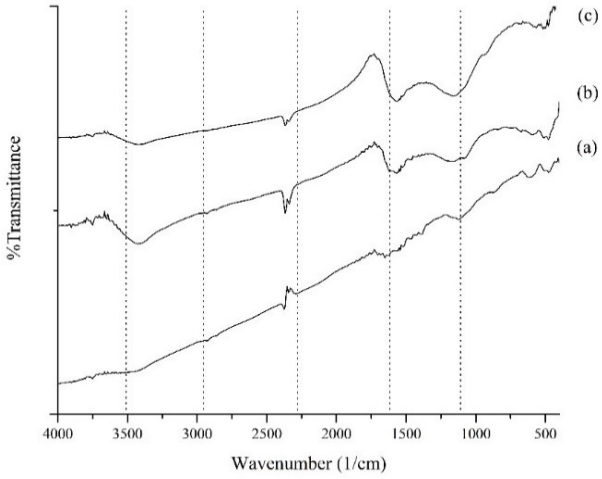

Figure 1. FTIR spectra of a) CAC, b) CPAC-201, and c) CPAC-202

Table 1. Functional groups of activated carbon

No.	Functional group	Wavenumber of activated carbon (cm^{-1})			
		Theoretical [27]	CAC	CPAC-201	CPAC-202
1	O–H	3570 – 3450	3510.45	3425.58	3425.58
2	C–H	2975 – 2915	2931.80	2931.80	2931.80
3	C≡C	2260 – 2190	2291.43	2337.72	2337.72
4	C=C	1660 – 1580	1635.64	1620.21	1620.21
5	C=N	1570 – 1515	-	1566.20	1566.20
6	C–O	1200 – 1050	1126.43	1157.29	1157.29

3.2. XRD Characterization of CPAC

The diffractogram of standard activated carbon (Figure 2a) shows the appearance of a wide angular range and the absence of sharp peaks in the activated carbon diffractogram, indicating the dominant structure is amorphous [25]. The diffractogram pattern of standard activated carbon shows two peaks at diffraction angles of ~24° and ~44° (weak) (Figure 2a).

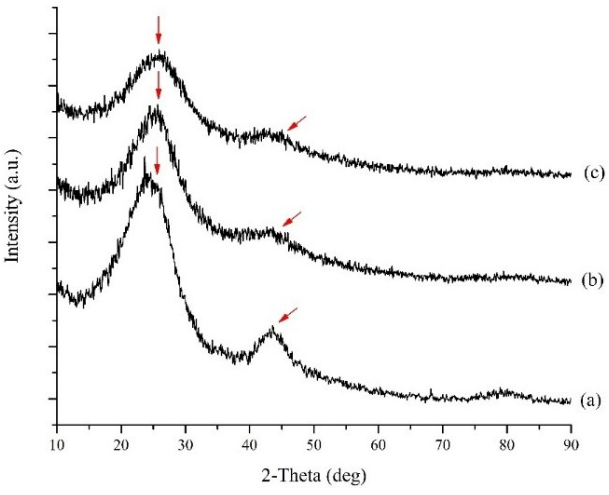

Figure 2. X-ray diffractogram of a) CAC, b) CPAC-201, and c) CPAC-202

The XRD patterns of CPAC-201 (Figure 2b) and CPAC-202 (Figure 2c) show two diffraction peaks at angles of ~25° (medium) and ~43° (weak). These results show a diffraction pattern similar to that of standard activated carbon (Figure 2a). Therefore, the preparation of CPAC without or with carbonization has no significant impact on the crystalline or amorphous character of the CPAC produced.

3.3. Surface and Pore Analysis of CPAC

In the surface analysis of CPAC-201 and CPAC-202, the results in Figures 3 and 4 show that the surface image in the process without carbonization (CPAC-201) is homogeneous and non-porous, while with carbonization (CPAC-202), it tends to be homogeneous, and pores are formed. In the elemental composition analysis, both CPAC surfaces are dominated by the element carbon (C), with a percentage exceeding 50% in both atomic and mass percentages. The presence of phosphorus (P) and sodium (Na) elements is expected due to the use of H_3PO_4 and NaOH in the process of making cassava peel-activated carbon. In Figure 4, a percentage of the element nitrogen (N) is presented, which supports the previous characterization data obtained using an FTIR spectrophotometer, showing the stretching vibrations of the C=N bond of the cyanide compound present in cassava peel.

The carbonization significantly impacts the pore properties of activated carbon materials, primarily influencing pore development, size, volume, and surface area. Carbonization promotes the release of volatile compounds, creating initial pores in the carbon structure. Efficient thermal decomposition of volatile matter increases surface area and micropore volume due to more complete carbonization [26]. Elevated carbonization temperatures tend to favor micropore and mesopore development, as more volatile components are removed, leading to increased pore volume and specific surface area [28].

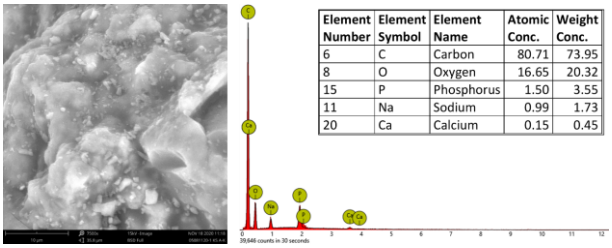

Element Number	Element Symbol	Element Name	Atomic Conc.	Weight Conc.
6	C	Carbon	80.71	73.95
8	O	Oxygen	16.65	20.32
15	P	Phosphorus	1.50	3.55
11	Na	Sodium	0.99	1.73
20	Ca	Calcium	0.15	0.45

Figure 3. SEM image and element composition on the CPAC-201 surface

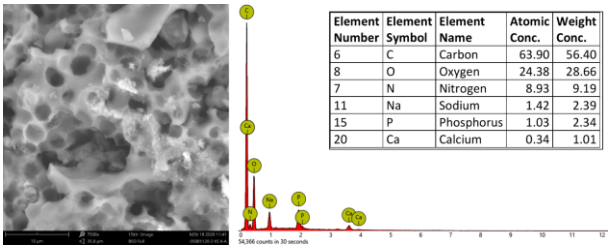

Element Number	Element Symbol	Element Name	Atomic Conc.	Weight Conc.
6	C	Carbon	63.90	56.40
8	O	Oxygen	24.38	28.66
7	N	Nitrogen	8.93	9.19
11	Na	Sodium	1.42	2.39
15	P	Phosphorus	1.03	2.34
20	Ca	Calcium	0.34	1.01

Figure 4. SEM image and element composition on the CPAC-202 surface

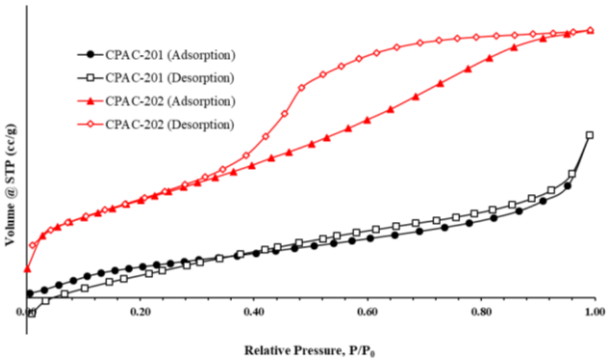

Figure 5. Nitrogen adsorption-desorption isotherm of CPAC samples

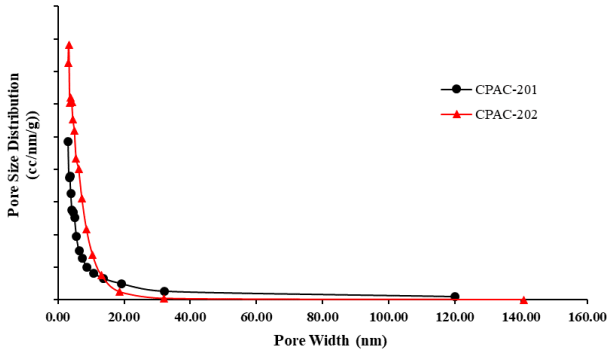

Figure 6. Pore size distribution of CPAC samples

CPAC samples, produced with and without carbonization, were analyzed using the BET method to determine surface area, pore characteristics (microporous or mesoporous), and total pore volume. The complete BET analysis results are presented in Figures 5 and 6, as well as in Table 2. The analysis was conducted based on nitrogen adsorption–desorption isotherms using relative pressure (P/P_0).

Based on Figure 5, CPAC-201 follows a type II isotherm plot, indicating predominantly non-porous or macroporous characteristics, whereas CPAC-202 follows a type IV isotherm associated with capillary condensation in mesopores and a limiting uptake at high P/P_0. CPAC-202 also exhibits a strong H2-type hysteresis loop, reflecting the differences between adsorption and desorption mechanisms in ink–bottle–type pores with narrow necks and wider bodies [29]. The H2 loop is associated with non-uniform, often irregular or elongated pores, with significant connectivity between pores, possibly forming a network that impacts fluid condensation and evaporation dynamics [30].

The pore characteristics of CPAC-201 and CPAC-202 show pore diameters in the nanoscale range (< 10 nm) (Figure 6). The average pore sizes are 3.84 nm for CPAC-201 and 2.28 nm for CPAC-202, placing both within the mesoporous category (2–50 nm) [31]. Additional parameters, including surface area and pore volume, are summarized in Table 2. However, CPAC-201 exhibits a very low surface area (4.773 m^2/g) and pore volume (0.009 cm^3/g), indicating weak mesoporosity, which is consistent with its type II isotherm behavior and suggests characteristics closer to those of non-porous or macroporous materials.

Table 2. BET surface areas and pore volumes of CPAC samples

Sample	S_{BET}[a] (m^2/g)	S_{mic}[b] (m^2/g)	S_{mes} (m^2/g)	V_t[c] (cm^3/g)	V_{mic}[b] (cm^3/g)	V_{mes} (cm^3/g)
CPAC-201	4.773	0.000	4.773	0.009	0.000	0.009
CPAC-202	198.233	0.000	198.233	0.227	0.000	0.227

[a] Specific surface area calculated by the BET method at P/Po = 0.05–0.30
[b] Micropore evaluated by *t*-plot method
[c] Total pore volume obtained from the single-point adsorption volume at P/Po = 0.995

Table 3. The adsorption of BTEX using CPAC

Sample	Concentration of adsorbed BTEX on CPAC (gas, mg/L)				
	Benzene	Toluene	Etil benzene	m,p-Xylene	o-Xylene
CPAC-201	0.262	1.273	0.264	1.799	0.580
CPAC-202	0.557	6.418	0.388	1.455	0.784

In contrast, CPAC-202 shows a significantly higher surface area of 198.233 m^2/g and a well-defined mesoporous structure (Figure 5). Li *et al.* [32] reported activated carbons with extremely high surface areas, reaching ~2,000 m^2/g, produced from biomass sources such as pine cones, spruce cones, larch cones, and whole spruce cones. These findings highlight that different biomass precursors can yield surface areas that vary widely. The final surface area is strongly influenced by factors such as biomass type, activation agent, activation temperature, and activation duration.

Overall, the pore characteristics obtained here show that the carbonization conditions applied to CPAC-202 were more effective in developing pore structures, resulting in a much larger surface area and a stronger mesoporous character.

3.4. Adsorption of BTEX

CPAC-201 and CPAC-202 were used as BTEX adsorbents at an initial concentration of 25 mg/L. The results showed that CPAC-201 achieved its highest adsorption with m,p-xylene (1.799 mg/L), while CPAC-202 showed its best performance with toluene (6.418 mg/L). These results indicate that activated carbon with a larger surface area and mesoporous character (CPAC-202) has better adsorption performance. This aligns with previous studies [33, 34], which reported that the BTEX adsorption process is strongly influenced by specific surface area, pore volume, and pore size. In this study, BTEX results were more dominant in CPAC-202, which has a larger surface area and pore volume capacity.

In the CPAC-202, the presence of C=N bonds on adsorbent surfaces generally enhances BTEX adsorption mainly through increased chemical interaction and affinity. The C=N functional groups (like amines) introduce basic sites and can form stronger interactions with the aromatic rings of BTEX by π-π electron donor-acceptor interactions or hydrogen bonding, increasing adsorption capacity [35]. The C=N groups can enhance surface polarity and selectivity, improving BTEX capture from gas or aqueous phases compared to non-functionalized carbons [36].

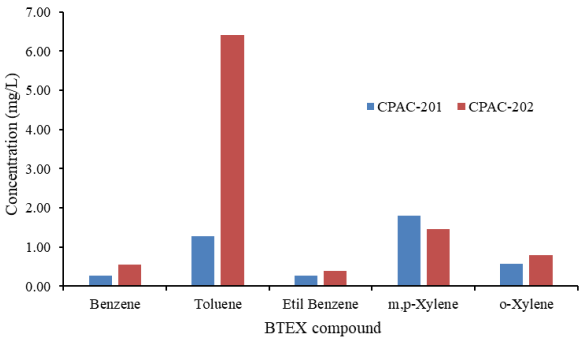

Figure 7. Adsorption of BTEX using CPAC samples

4. Conclusion

Activated carbon from cassava peels (CPAC) was successfully synthesized through carbonization at 400°C (t: 60 minutes) followed by a dual activation stage: chemical activation (carbon: 30% H_3PO_4, ratio 1:5, w/w) and physical activation (furnace, T: 600°C, t: 60 minutes). The activated carbon derived from biomass, such as cassava peels, is highly regarded for its renewability and environmental friendliness (SDGs 11, 13, and 15). CPAC-201 (without carbonization) and CPAC-202 (with carbonization) have an amorphous character with functional groups that include O-H, C-H, C≡C, C=C stretching, C-O, and C=N. In the SEM-EDX section results, the surfaces of CPAC-201 and CPAC-202 are dominated by C and O elements, with a porous surface character observed on CPAC-202. The carbonization step changes pore properties. CPAC-202 (with carbonization) has a mesoporous character with a surface area up to 198.233 m^2/g, and the surface is dominated by C and O elements. The selectivity of BTEX gas adsorption is more significant for toluene using CPAC-202, with the best adsorption reaching 6.418 mg/L.

Acknowledgments

Researchers would like to thank Satya Wacana Christian University (Salatiga, Indonesia) for providing funding assistance to purchase materials and characterize instruments in this research through the UKSW Fundamental Research Grant scheme for the Fiscal Year from July to December 2020.

References

[1] Margaret O. Ilomuanya, Billa Nashiru, Ndu D. Ifudu, Cecilia I. Igwilo, Effect of pore size and morphology of activated charcoal prepared from midribs of *Elaeis guineensis* on adsorption of poisons using metronidazole and *Escherichia coli* O157:H7 as a case study, *Journal of Microscopy and Ultrastructure*, 5, 1, (2017), 32-38 https://doi.org/10.1016/j.jmau.2016.05.001

[2] Muniandy Gayathiri, Thiruchelvi Pulingam, K. T. Lee, Kumar Sudesh, Activated carbon from biomass waste precursors: Factors affecting production and adsorption mechanism, *Chemosphere*, 294, (2022), 133764 https://doi.org/10.1016/j.chemosphere.2022.133764

[3] J. U. Ani, K. G. Akpomie, U. C. Okoro, L. E. Aneke, O. D. Onukwuli, O. T. Ujam, Potentials of activated carbon produced from biomass materials for sequestration of dyes, heavy metals, and crude oil components from aqueous environment, *Applied Water Science*, 10, 2, (2020), 69 https://doi.org/10.1007/s13201-020-1149-8

[4] K. M. Oghenejoboh, Effects of Cassava Wastewater on the Quality of Receiving Water Body Intended for Fish Farming, *Current Journal of Applied Science and Technology*, 6, 2, (2014), 164–171 https://doi.org/10.9734/BJAST/2015/14356

[5] Estêvão A. Pondja Jr., Kenneth M. Persson, Nelson P. Matsinhe, The Potential Use of Cassava Peel for Treatment of Mine Water in Mozambique, *Journal of Environmental Protection*, 8, 03, (2017), 277 https://doi.org/10.4236/jep.2017.83021

[6] Sonny Widiarto, Edi Pramono, Suharso, Achmad Rochliadi, I Made Arcana, Cellulose nanofibers preparation from cassava peels via mechanical disruption, *Fibers*, 7, 5, (2019), 44 https://doi.org/10.3390/fib7050044

[7] Syazwani Mohd-Asharuddin, Norzila Othman, Nur Shaylinda Mohd Zin, Husnul Azan Tajarudin, A Chemical and Morphological Study of Cassava Peel: A Potential Waste as Coagulant Aid, *International Symposium on Civil and Environmental Engineering 2016 (ISCEE 2016)*, 2017 https://doi.org/10.1051/matecconf/201710306012

[8] Qi Wang, Bolong Luo, Zhaoyu Wang, Yao Hu, Mingliang Du, Pore engineering in biomass-derived carbon materials for enhanced energy, catalysis, and environmental applications, *Molecules*, 29, 21, (2024), 5172 https://doi.org/10.3390/MOLECULES29215172

[9] E. Menya, P. W. Olupot, H. Storz, M. Lubwama, Y. Kiros, Production and performance of activated carbon from rice husks for removal of natural organic matter from water: A review, *Chemical Engineering Research and Design*, 129, (2018), 271-296 https://doi.org/10.1016/j.cherd.2017.11.008

[10] Ibsa Neme, Girma Gonfa, Chandran Masi, Activated carbon from biomass precursors using phosphoric acid: A review, *Heliyon*, 8, 12, (2022), e11940 https://doi.org/10.1016/j.heliyon.2022.e11940

[11] Guilaine Jaria, Vânia Calisto, Valdemar I. Esteves, Marta Otero, Overview of relevant economic and environmental aspects of waste-based activated carbons aimed at adsorptive water treatments, *Journal of Cleaner Production*, 344, (2022), 130984 https://doi.org/10.1016/j.jclepro.2022.130984

[12] S. M. Yakout, G. Sharaf El-Deen, Characterization of activated carbon prepared by phosphoric acid activation of olive stones, *Arabian Journal of Chemistry*, 9, (2011), S1155-S1162 https://doi.org/10.1016/j.arabjc.2011.12.002

[13] Walny Nicha, Mohammad Wijaya M., Hasri Hasri, Synthesis and Characterization of Palm Shell Activated Carbon for Adsorption of Remazol Brilliant Violet 5R, *Jurnal Kimia Sains dan Aplikasi*, 28, 8, (2025), 405-415 https://doi.org/10.14710/jksa.28.8.405-415

[14] Joseph Jjagwe, Peter Wilberforce Olupot, Emmanuel Menya, Herbert Mpagi Kalibbala, Synthesis and Application of Granular Activated Carbon from Biomass Waste Materials for Water Treatment: A Review, *Journal of Bioresources and Bioproducts*, 6, 4, (2021), 292-322 https://doi.org/10.1016/j.jobab.2021.03.003

[15] Amphol Aworn, Paitip Thiravetyan, Woranan Nakbanpote, Preparation and characteristics of agricultural waste activated carbon by physical activation having micro- and mesopores, *Journal of Analytical and Applied Pyrolysis*, 82, 2, (2008), 279-285 https://doi.org/10.1016/j.jaap.2008.04.007

[16] Abdel-Nasser A. El-Hendawy, S. E. Samra, B. S. Girgis, Adsorption characteristics of activated carbons obtained from corncobs, *Colloids and Surfaces A: Physicochemical and Engineering Aspects*, 180, 3, (2001), 209-221 https://doi.org/10.1016/S0927-7757(00)00682-8

[17] Roba M. Almuhtaseb, Sneha Bhagyaraj, Igor Krupa, A concise review on BTEX remediation from aqueous solutions by adsorption, *Emergent Materials*, 7, 3, (2024), 695-719 https://doi.org/10.1007/S42247-024-00640-1

[18] Wenjuan Wu, Kai Cheng, Yeye Hu, Han He, Pan Wang, Chengzhu Zhu, Adsorption and desorption mechanism of toluene gas by iron modified activated carbon fiber, *Chemical Physics*, 580, (2024), 112240 https://doi.org/10.1016/j.chemphys.2024.112240

[19] Aminu Ibrahim, Azimah Ismail, Hafizan Juahir, Mark Ovinis, Yudi Nurul Ihsan, Sunardi Sudianto, Azlina Md Kassim, BTEX adsorption from aqueous solutions using activated carbon from *Melaleuca cajuputi* leaves, *Kuwait Journal of Science*, 51, 4, (2024), 100247 https://doi.org/10.1016/j.kjs.2024.100247

[20] Leili Mohammadi, Edris Bazrafshan, Meissam Noroozifar, Alireza Ansari-Moghaddam, Farahnaz Barahuie, Davoud Balarak, Adsorptive Removal of Benzene and Toluene from Aqueous Environments by Cupric Oxide Nanoparticles: Kinetics and Isotherm Studies, *Journal of Chemistry*, 2017, 1, (2017), 2069519 https://doi.org/10.1155/2017/2069519

[21] Tri Ariyanto Nugroho, Cucun Alep Riyanto, November Rianto Aminu, Adsorption of Cadmium (II) Ions Using Cassava Peel Activated Carbon: Study of Adsorption Kinetics, Isotherms and Thermodynamics, *Indonesian Journal of Chemical Analysis (IJCA)*, 7, 1, (2024), 12-22 https://doi.org/10.20885/ijca.vol7.iss1.art2

[22] Cucun A. Riyanto, Alvama Pattiserlihun, Ezra Kurniawan, Blessy Y. Andiani, Fahmi P. Perdani, Surface analysis of activated carbon from rice husk based on carbonization and activation method, *AIP Conference Proceedings*, 2542, 1, (2022), 020005 https://doi.org/10.1063/5.0103325

[23] Fahmi Puteri Perdani, Cucun Alep Riyanto, Yohanes Martono, Karakterisasi Karbon Aktif Kulit Singkong (*Manihot esculenta* Crantz) Berdasarkan Variasi Konsentrasi H_3PO_4 dan Lama Waktu Aktivasi, *Indonesian Journal of Chemical Analysis (IJCA)*, 4, 2, (2021), 72-81 https://doi.org/10.20885/ijca.vol4.iss2.art4

[24] Blessy Yemima Andiani, Cucun Alep Riyanto, Yohanes Martono, Characterization of Cassava (*Manihot esculenta* Crantz) Peel Activated Carbon based on Impregnation Ratio and Activation Temperature: Karakterisasi Karbon Aktif Kulit Singkong (*Manihot esculenta* Crantz) Berdasarkan Rasio Impregnasi dan Suhu Aktivasi, *Stannum : Jurnal Sains dan Terapan Kimia*, 4, 1, (2022), 19-26 https://doi.org/10.33019/jstk.v4i1.2533

[25] Lok Kumar Shrestha, Laxmi Adhikari, Rekha Goswami Shrestha, Mandira Pradhananga Adhikari, Rina Adhikari, Jonathan P. Hill, Raja Ram Pradhananga, Katsuhiko Ariga, Nanoporous carbon materials with enhanced supercapacitance performance and non-aromatic chemical sensing with C_1/C_2 alcohol discrimination, *Science and Technology of Advanced Materials*, 17, 1, (2016), 483-492 https://doi.org/10.1080/14686996.2016.1219971

[26] E. Budi, H. Nasbey, B. D. P. Yuniarti, Y. Nurmayatri, J. Fahdiana, A. S. Budi, Pore structure of the activated coconut shell charcoal carbon, *AIP Conference Proceedings*, 1617, 1, (2014), 130-133 https://doi.org/10.1063/1.4897121

[27] B. D. Mistry, *A Handbook of Spectroscopic Data Chemistry: (UV, IR, PMR, 13CNMR and Mass Spectroscopy)*, Oxford Book Company, 2009,

[28] Shijie Li, Xiaopeng Tan, Hui Li, Yan Gao, Qian Wang, Guoning Li, Min Guo, Investigation on pore structure regulation of activated carbon derived from sargassum and its application in supercapacitor, *Scientific Reports*, 12, (2022), 10106 https://doi.org/10.1038/s41598-022-14214-w

[29] K. S. W. Sing, Reporting physisorption data for gas/solid systems with special reference to the determination of surface area and porosity (Recommendations 1984), *Pure and Applied Chemistry*, 57, 4, (1985), 603-619 https://doi.org/10.1351/pac198557040603

[30] Nadiya B. Nayak, Bibhuti B. Nayak, Temperature-mediated phase transformation, pore geometry and pore hysteresis transformation of borohydride derived in-born porous zirconium hydroxide nanopowders, *Scientific Reports*, 6, 1, (2016), 26404 https://doi.org/10.1038/SREP26404

[31] Nils Carlsson, Hanna Gustafsson, Christian Thörn, Lisbeth Olsson, Krister Holmberg, Björn Åkerman, Enzymes immobilized in mesoporous silica: A physical–chemical perspective, *Advances in Colloid and Interface Science*, 205, (2014), 339-360 https://doi.org/10.1016/j.cis.2013.08.010

[32] Gui Li, Artem Iakunkov, Nicolas Boulanger, Oana Andreea Lazar, Marius Enachescu, Alejandro Grimm, Alexandr V. Talyzin, Activated carbons with extremely high surface area produced from cones, bark and wood using the same procedure, *RSC Advances*, 13, 21, (2023), 14543-14553 https://doi.org/10.1039/D3RA00820G

[33] Abbas Aleghafouri, Nadia Hasanzadeh, Mohammad Mahdyarfar, Aliakbar SeifKordi, Seyed Morteza Mahdavi, Ali Taghi Zoghi, Experimental and theoretical study on BTEX removal from aqueous solution of diethanolamine using activated carbon adsorption, *Journal of Natural Gas Science and Engineering*, 22, (2015), 618-624 https://doi.org/10.1016/j.jngse.2015.01.010

[34] Maria Luisa Feo, Massimiliano Frattoni, Ester Paoloacci, Maria Masiello, Giulio Esposito, Rafael Gonzalez-Olmos, Emanuela Tempesta, Francesca Trapasso, Emiliano Zampetti, Marco Torre, Ettore Guerriero, Valerio Paolini, Assessing the efficiency of zeolites in BTEX adsorption: Impact of pore structure and humidity in single and multicomponent systems, *Microporous and Mesoporous Materials*, 384, (2025), 113462 https://doi.org/10.1016/j.micromeso.2024.113462

[35] Luyu Wang, Xiaoli Cha, Yunling Wu, Jin Xu, Zhixuan Cheng, Qun Xiang, Jiaqiang Xu, Superhydrophobic Polymerized *n*-Octadecylsilane Surface for BTEX Sensing and Stable Toluene/Water Selective Detection Based on QCM Sensor, *ACS Omega*, 3, 2, (2018), 2437-2443 https://doi.org/10.1021/acsomega.8b00061

[36] Christian F. Varela, M. Carolina Pazos, María D. Alba, Organophilization of acid and thermal treated sepiolite for its application in BTEX adsorption from aqueous solutions, *Journal of Water Process Engineering*, 40, (2021), 101949 https://doi.org/10.1016/j.jwpe.2021.101949